International Journal of Fluid Machinery and Systems
Vol. 6, No. 4, October-December 2013

DOI: http://dx.doi.org/10.5293/IJFMS.2013.6.4.189
ISSN (Online): 1882-9554

Original Paper

Development of a Simulation Method of Surge Transient Flow Phenomena in a Multistage Axial Flow Compressor and Duct System

Nobuyuki Yamaguchi

Meisei University (retired)
Aoba-ku, Akanedai, 2-1-25, Yokohama City, 227-0066, Japan
yamaguchi_nandm@hb.tp1.jp

Abstract

A practical method of surge simulation in a system of a high-pressure-ratio multistage axial flow compressor and ducts, named SRGTRAN, is described about the principal procedures and the details. The code is constructed on the basis of one-dimensional stage-by-stage modeling and application of fundamental equations of mass, momentum, and energy. An example of analytical result on surge behaviors is included as an experimental verification. It will enable to examine the transient flow phenomena caused by possible compressor surges and their influences on the system components in plant systems including high-pressure-ratio axial compressors or gas turbines.

Keywords: Fluid Machine, Axial Flow Compressor, Surge, Fluid Dynamics, Analytical Simulation, Transient Flow

1. Introduction

High-pressure-ratio axial flow compressors have been employed in many applications of high power output, such as jet engines, gas turbines, industrial air sources, etc. With the advent of the environmental ages, they will be utilized further in various types of advanced combined-cycle plants using gas turbines as high-temperature core components. If a surging happens to occur in spite of various surge-preventive measures, violent waves and oscillations of flow could propagate both upstream and downstream in the system, having possibly adverse influences on the structural and operational safety of the system and structures. The waves could include various multi-scale phenomena, such as surge waves, sudden stop and possible reversal of the air flow, possible back-fire of burning gases accompanying very high temperature, abrupt positive and negative pressure changes resulting from surge hammer-shocks, rotating stalls, and local waves, etc. Stall stagnation phenomena could occur depending on the situations. They could occur nearly simultaneously over the whole ducts and compressor passages. Thus surge and post-stall behaviors of the flows in compressors and flow-paths have been and should be paid attention to.

In this context, it is required to make clear and evaluate quantitatively the phenomena accompanied by the surging. For the purpose, it is necessary to treat the large-amplitude transient phenomena distributed over the whole flow-path and related components. Furthermore, it should be reasonably taken into consideration that significant mismatching of stage operating points in the off-design conditions caused by the flow compressibility effects could complicate the surge phenomena particularly in the high-pressure-ratio multi-stage compressor environments.

The principle of the surge phenomena in pump systems was clarified as early as 1947 by Fujii[1]. The self-excited nature of the surges has been clarified in principle by his formulation and graphical solutions. In 1960, Katto [2] investigated on resonant surges in systems of a low-pressure axial flow fan and ducts and studied the phenomena experimentally and theoretically using electric circuit analogy and phase analysis.

In 1976, Greitzer[3] formulated the situation by a simplified lumped-parameter model of a system of a low-pressure compressor and a plenum and made clear the surge transient behaviors by numerical calculations. He has found his B parameter as an important controlling parameter in the surge behaviors. It determines whether the system maintains a deep surge condition or decays into a stagnation stall condition. Since then, the B parameter has been extensively used in various field of present-day surge technology, for example, in the study of active stall control.

Received May 31 2013; revised June 29, September 26 2013; accepted for publication September 27 2013: Review conducted by Dr. Hideaki Tamaki. (Paper number O13025C)
Corresponding author: Nobuyuki Yamaguchi, yamaguchi_nandm@hb.tp1.jp

In 1970's and 1980's, basic mathematical modelings of multistage axial flow compressors in surge, which are reasonable from the fluid-dynamic point of view, were proposed by Corbett and Elder [4], Chamblebee, Davies, Jr., and Kimzey [5], Davies, Jr. and O'Brien [6], etc. Several studies on jet engine compressors have been reported by them. The methods were innovative in that they treated the flow situation as a distributed-parameter system in the compressor stages and over the whole flow-path, distinct from the preceding lumped parameter ones using such as actuator discs and concentrated volumes. They were promising from the practical and engineering point of view in the environment affected significantly by multi-stage effects and compressibility effects.

In 1990's and 2000's, utilization of these basic techniques of mathematical modeling have been widening to dynamic simulation of a whole plant or system of turbomachines, such as gas turbines, jet engines, compressor plants, including machine dynamics (for example, Schobeiri, etc. [7], Badmus, etc. [8], Schobeiri [9], etc.).

The author as a compressor engineer has long been concerned with and interested in compressor surge problems. So, he has become keenly aware of the necessity of constructing a practical tool for study of various phenomena of surge in the environment of high-pressure-ratio and large-capacity multi-stage compressors integrated into complicated flow- paths. For the purpose, the author has been trying to prepare such a code, named SRGTRAN. In his previous papers (Yamaguchi [10, 11]) on stall stagnation boundary, although the contents have been based on the analytical results derived by use of SRGTRAN, the details of the method could not have been included there because of the space limitations. The author wishes to describe about the SRGTRAN here, though it is not in the right order.

2. Flow chart of SRGTRAN

Figure 1 shows a rough flow chart of the procedures in SRGTRAN. The code is programmed for use on a personal computer.

The whole flow-path consisted of the upstream duct, the compressor stages and the downstream duct is divided into a series of control volumes (CVs), the number of which should be sufficient for describing reasonably the local conditions of the path geometry and the flow conditions, as shown in Section 3.

The first step of the analysis is the steady-state evaluation of the flow conditions in the compressor and the duct immediately before the stalling of a most-impending stage in the compressor. It uses a conventional method of one-dimensional stage-by-stage performance estimation based on the stage characteristics data concerning pressure coefficient and temperature coefficient vs. flow coefficient. It sets the starting condition of the surge transient evaluation. At this stage, it is necessary to fix the time step Δt on the basis of CFL (Courant-Friedrics-Lewy) condition (*cf.* Ref [12]), and, at the same time, to determine the valve opening area *Av* that allows to pass the stalling mass flow under the corresponding pressure difference across the valve.

The stage characteristics require data over a very wide range of flow coefficient covering a turbine-action zone to the reversed flow zone. Data on the characteristics are required to be reliable as far as possible for reasonable estimation of the surge behaviors if possible, though difficult to obtain in many cases.

Then, the transient analysis is started at time t =0 from the initial steady-state data on the whole flow path conditions to determine the data for time $t = \Delta t$. The process is repeated similarly from the conditions at $t = k\Delta t$ to the ones at time $t = (k+1)\Delta t$.

This code employs the two-stage Lax-Wendroff method (*cf.* Ref [12]) for the compressor stage flow-path s and the method of characteristics for the duct flow-paths upstream and downstream. The former method is suitable particularly in the compact space of compressor stages where significant changes in conditions of flow, forces and energies could occur in a rather concentrated manner. The method of characteristics is convenient in relatively slowly changing situations in the flow conditions and the flow-path geometry. It is both stable in calculation process and accurate in specifying the boundary condition at the duct end. The formulation by Tanahashi [13] is employed here.

Boundary conditions at the valve are essential also. Here the transient valve flow is approximately formulated and employed as given later.

Further detailed information about the code is given below.

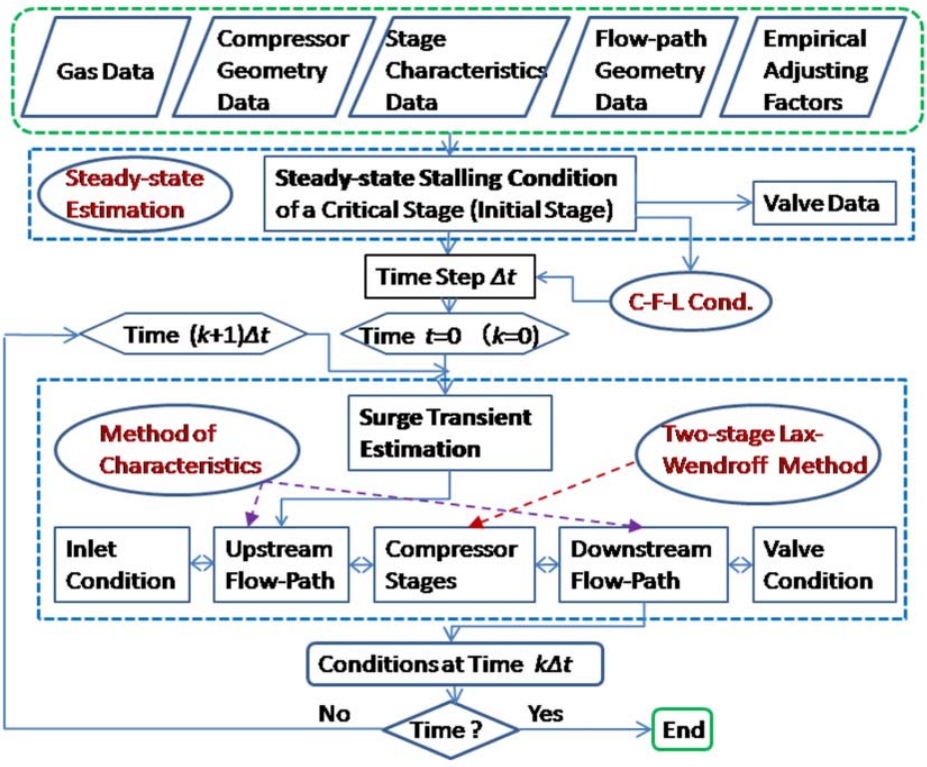

Fig. 1 Rough flow chart of SRGTRAN

3. Modeling of a compressor and duct system

SRGTRAN has employed the following system of analysis. Flow behaviors within the compressor and the duct system are expressed as functions of (x, t) where x is one-dimensional space coordinate in the axial direction, and t means time. Here, the phenomena only in the axial-direction are considered. Effects of swirling flow components and rotating stalls on the surge phenomena are assumed to be relatively small.

3.1 CVs for the duct flow-path

The flow- path is divided into a suitable number of control volumes (CVs) as shown in Fig.2. In each CV, the method of characteristics is applied and the variables are connected continuously to those in both neighboring CVs at the respective connecting surfaces. The numbers of CVs and the CV inlet are given by integer i in a manner as follows; i=iI=1: the inlet of the whole duct, i=iE-1: the last CV of the whole duct, i=iE: the exit of the last CV, i=iC - iC+1: occupied by the compressor, where at iC and iC+1, the inlet of the compressor first stage and the exit of the last stage are located, respectively. The internals of the compressor are represented by another numbering system described in Section 3.2. An exit valve is mounted at the section iE.

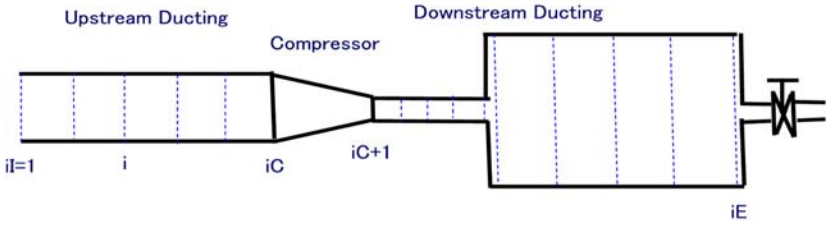

Fig. 2 Control volumes and numbering for a compressor-ducting system

3.2 Compressor flow-path

Figure 3 shows basic control volumes (CVs) in the compressor flow-path. Each stage consisted of a rotor row and a stator row forms a basic control volume, CV. The control surfaces at the inlet and the exit of each CV correspond to the upstream section and the downstream one of the stage, and have location indices “1” and ” 2”, respectively. Index “m” means the intermediate section or the average position. The section indices are used as suffices for flow variables. The stage number “J” or “j” is used in combination.

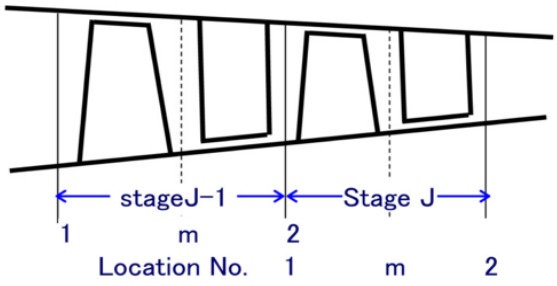

Fig. 3 Constitution of a compressor stage and numbering of the locations

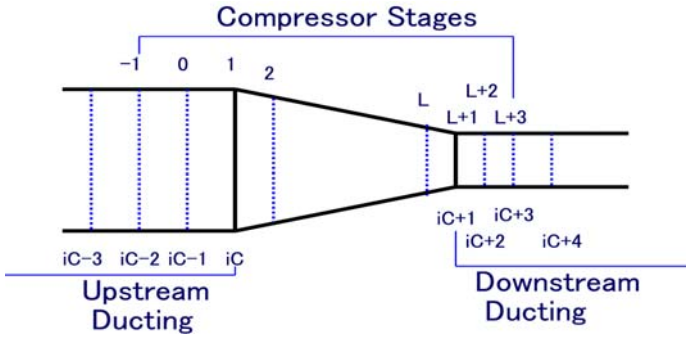

Fig. 4 Superposition of the compressor inlet and exit and the duct control volumes

3.3 Connection between the compressor and the duct

For connecting the flow-paths between the ducts and the compressor, as shown in **Fig. 4,** two empty stages are added both upstream and downstream of the compressor, respectively. The empty stages are calculated at the same time by the two different method described above in an overlapped manner. The continuity of the flow conditions at the interfaces are secured by matching both results among them.

4. Flow Dynamics in the Compressor

4.1 Flow Conditions in Compressor Stages

Time t is expressed by integer number k as follows;

$$t = k\Delta t \qquad (1)$$

Here, Δt is a time step for the calculation.

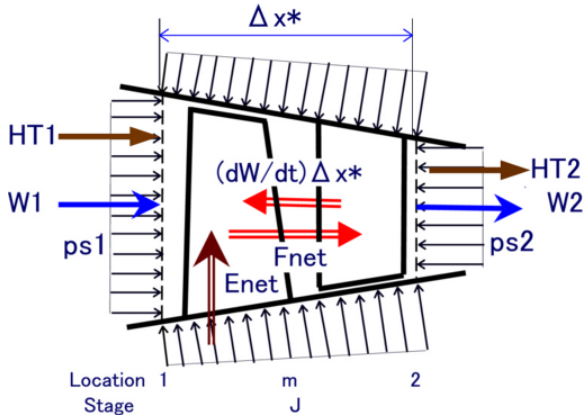

Fig. 5 Control volume and conditions of a compressor stage

Figure 5 shows a CV together with the situation concerning mass flows, forces and energies into and out of the stage CV. Here, Δx^* means the axial length of the CV, and the sectional area of the CV or the stage annulus passage is A.

4.2 Basic Equations

The flow dynamics with respect to the CV given in Fig. 5 follows the mathematical modeling technique given by Corbett and Elder [4], Chamblebee, Davies, Jr., and Kimzey [5], Davies, Jr. and O'Brien [6], etc. Following three relations describe the flow behaviors in a CV. Suffices 1, 2, and m show conditions at the inlet, the exit and the mid-position of the CV, respectively.

(1) Conservation of mass in the CV The following relation results from the mass flows entering and leaving the CV and the mass stored within the CV shown in Fig. 5.

$$\frac{\partial \rho_m}{\partial t} = -\frac{1}{A_m}\frac{\partial W}{\partial x} \tag{2}$$

Here, W: mass flow (kg/s), ρ_m: average flow density in the CV (kg/m^3), A_m: the average flow-path area of the CV (m^2). The relation is valid as far as the annulus area change through the stage is relatively small. A bleed flow, if present, could be taken into consideration, if the corresponding term is added to the formulation.

(2) Conservation of momentum in the CV The following relation results from the momentums entering and leaving the CV and the forces acting on the CSs and within the CV shown in Fig. 5. The forces include the blade axial forces, inertial force of the contained fluid, pressure forces on the CS, etc. Here, CS means a control surface of the CV.

$$\frac{\partial W_m}{\partial t} = -\frac{\partial}{\partial x}\left(Wu + p_s A\right) + \frac{Fnet - \frac{1}{2}\left(p_{s1} + p_{s2}\right)\left(A_1 - A_2\right)}{\Delta x^*} \tag{3}$$

Here, u: axial velocity of the flow (m/s), ps: static pressure (Pa), $Fnet$: net axial force of the stage resulting from the axial components of pressures and drags distributed over the blades. Δx^* means the axial length of the stage or the CV.

(3) Conservation of energy in the CV The following relation results from the total enthalpies H_{T1} and H_{T2} entering and leaving the CV and the internal energy within the CV and the work done by the stage shown in Fig. 5.

$$\frac{\partial}{\partial t}\left[\rho_m\left(C_V T_{sm} + \frac{1}{2}u_m^2\right)\right] = -\frac{1}{A_m}\frac{\partial}{\partial x}\left(C_P T_T W\right) + \frac{Enet}{A_m \Delta x^*} \tag{4}$$

Here, Cp: specific heat at constant pressure (J/kg/K), Cv: specific heat at constant volume (J/kg/K), T_T: total temperature (K), T_S: static temperature (K), u_m : average flow velocity (m/s). *Enet:* net energy given to the flow, including the increase in the total enthalpy by the stage work, contribution from the heat addition or absorption from outside, etc. Energy removal by a bleed flow, if present, could be taken into consideration, if the corresponding term is added to the formulation.

The second groups of terms in the right- hand side of Eqs. (3) and (4) treat the stage forces and the stage works as uniformly distributed source terms, respectively.

4.3 Working conditions, stage forces and stage works The transient stage conditions are determined from the steady-state stage conditions through the performance characteristics as follows;

(1) Basic stage characteristics The stage characteristics are given by the following steady-state parameters .

Flow coefficient

$$\phi = u_m / U_{ref} \tag{5}$$

Pressure coefficient

$$\psi_P = \frac{C_P T_{T1}\left[\left(P_{T2}/P_{T1}\right)^{\{(\kappa-1)/\kappa\}} - 1\right]}{(1/2)U_{ref}{}^2} \tag{6}$$

Temperature Coefficient

$$\psi_T = C_P\left(T_{T2} - T_{T1}\right)\Big/(1/2)U_{ref}{}^2 \tag{7}$$

Here, u_m: annulus-averaged axial flow velocity (m/s), U_{ref}: reference peripheral speed of the compressor blade (m/s), T_{T1} and T_{T2}: total temperature at the stage inlet and the stage exit (K), respectively, P_{T1} and P_{T2}: total pressure at the stage inlet and the stage exit (Pa), respectively, and κ : ratio of specific heats.

The stage characteristics are required to cover a very wide range of flow from the large flow turbine-action zone to the reversed flow zone. Such wide-range characteristics are ordinarily difficult to obtain at present. It would be necessary to suppose or extrapolate on the basis of some related experimental data, especially in the reversed flow zone. For example, Greitzer [3], Gamache and Greitzer [15], Day, Greitzer, and Cumpsty [16], Davis, Jr. and O'Brien [6], etc. should be referred to. Some relevant data derived from multistage situations could be useful also, in such as Hosny and Steenken [17], Boyer and O'Brien [18], and Copenhaver and Okiishi [19]. An estimation method of wide-range stage characteristics constructed by simplified modeling of the respective zones of the stage flow situations in Bloch and O'Brien [20] could also be useful.

(2) Reference working conditions of a stage Reference working conditions of the stage are hypothetical steady-state ones

that could be realized after a lapse of long time for a fixed mass flow condition W_m, which is corresponding to the current mass flow at the time and at the mid-position "m" of the CV or the stage. The current mass flow W_m and the flow conditions give the mean axial velocity u_m of the stage or the average of the upstream and downstream values of the stage.

$$u_m = W_m \Big/ k_{bk} \rho_m A_m \tag{8}$$

Here, k_{bk}: blockage factor of the stage annulus passage, suffix m: the mid-position of the CV or the average condition of the quantity. It would be better to provide reasonable values of the blockage factor compatible with those in the steady-state performance calculations. The flow coefficient ϕ_m thus evaluated by Eq. (5) gives the corresponding values of the coefficients of pressure and temperature in reference to the prepared data of the stage characteristics. Thus, for the mass flow W_m throughout the stage, the downstream flow conditions of total pressure and total temperature can be estimated by use of Eqs. (6) and (7) from the known upstream flow conditions. Then the total conditions are converted to static conditions in a conventional manner. In the process, iterative calculations could be often required. In the reversed flow conditions, the procedure could be changed according to the definitions of the stage characteristics.

(3) Reference stage force and stage work On the basis of the above reference working conditions, the steady-state values of the net stage force *Fnet** and the net stage work *Enet** are evaluated by use of the ordinary steady-state relations compatible with Eqs. (3) and (4) as follows.

$$Fnet^* = W_m(u_2 - u_1) + (p_{s2} - p_{s1})(A_1 + A_2)/2 \tag{9}$$

$$E^*_{net} = C_P W_m (T_{T2} - T_{T1}) \tag{10}$$

Here, superscript * means the evaluated steady-state values.

If heating or cooling and works other than the stage works are present, they should be included in the above relations.

(4) Transient-state evaluation The actual transient stage force and work at time $k\Delta t$ will be realized in the course of heading toward the hypothetical values at time $k\Delta t$ from the past ones at time $(k\text{-}1)\Delta t$ with respective time lags τ_{lagP} and τ_{lagT} as follows.

$$F_{net}(k) = F_{net}(k-1) + \{F^*_{net}(k) - F_{net}(k-1)\}[1 - \exp(-\Delta t / \tau_{lagP})] \tag{11}$$

$$E_{net}(k) = E_{net}(k-1) + \{E^*_{net}(k) - E_{nety}(k-1)\}[1 - \exp(-\Delta t / \tau_{lagT})] \tag{12}$$

Here, k: present time, and k-1: time preceding by Δt.

4.4 Determination of time step Δt

In order to maintain a stable calculation, the time step Δt is required to satisfy the Courant-Friedrics-Lewy (CFL) condition (*cf.* Ref.[12]), namely,

$$T_{adj} = (|u| + a)\Delta t / \Delta x < 1 \tag{13}$$

Here, a: speed of sound, Δx: axial length of the CV, and Δt: calculation time step. In this procedure, in order to specify *Tadj* for the most critical CV, related parameters computed in the initial steady-state calculation are used.

From trials of several examples, the following order of magnitude of *Tadj* was found to be sufficient here.

$$Tadj \sim 0.2 \tag{14}$$

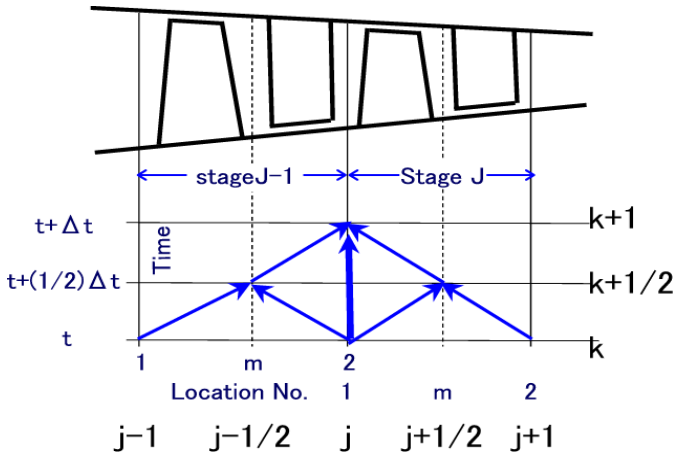

Fig. 6 Scheme employed for the two-stage Lax-Wendroff method

4.5 Stage calculations according to two-stage Lax-Wendroff method

It is necessary to compute the above relations in both x and t directions. According to the ordinary Lax method, the results on the pressures and mass flows, etc. have tended to oscillate and diverge in the long run of the computation. In order to suppress the adverse tendency, the two-stage Lax-Wendroff method (*cf.* Ref. [12]) has been employed. It is said that the two-stage Lax-Wendroff method has the accuracy of the second order of Δt and Δx.

Equations (2-4) are seen to have a common form of the following type.

$$\frac{\partial u}{\partial t} = b - \frac{\partial f}{\partial x} \tag{15}$$

Here, u, b, and f are vector representation of the variables appearing in Eqs. (2-4) and these symbols are defined and used only in this section (u does not mean axial velocity here). For the relations, the two-stage Lax-Wendroff method evaluates the conditions at time (k+1) from the ones at time k according to the following procedure. As seen in Fig.6, j and k are integers representing the space step and time step, respectively. In the compressor flow-path the inlet and the exit of stage J is named j and j +1, respectively. Points 1, m, and 2 of stage J are corresponding to points j, j+1/2, and j+1 in space, respectively, and time t, t +(1/2) Δt , and $t + \Delta t$ are corresponding to points k, k+1/2, and k+1 in time, respectively. From points (j -1, k), (j, k), and (j +1, k), evaluations at points (j -1/2, k+1/2) and (j +1/2, k+1/2) are obtained by the first stage. From points (j -1/2, k+1/2), (j +1/2, k+1/2), and (j, k), evaluations at point (j, k+1) is obtained by the second stage.

For the first stage of calculation,

$$u_{j+1/2}^{k+1/2} = \frac{1}{2}\left(u_{j+1}^{k} + u_{j}^{k}\right) - \frac{\Delta t}{2\Delta x}\left(f_{j+1}^{k} - f_{j}^{k}\right) + \frac{\Delta t}{4}\left(b_{j}^{k} + b_{j+1}^{k}\right) \tag{16}$$

For the second stage of calculation,

$$u_{j}^{k+1} = u_{j}^{k} - \frac{\Delta t}{\Delta x}\left(f_{j+1/2}^{k+1/2} - f_{j-1/2}^{k+1/2}\right) + \frac{\Delta t}{2}\left(b_{j+1/2}^{k+1/2} + b_{j-1/2}^{k+1/2}\right) \tag{17}$$

5. Flow Dynamics in the Duct Flow-paths

5.1 Duct Flow

For the analyses of the duct system except the compressor bladed flow-path, the method of characteristics is employed. It has been established methodologically (*cf.* Tanahashi [13]) and has merits of simplicity and stability in the calculation and of convenience in specifying the boundary conditions. It is suitable to the analysis of the duct flow-paths where changes in the conditions such as pressure and mass flow, and works and energies are much slower along the duct axis in comparison with the compressor flow-path. It could allow relatively sparse and not-regular layout of the CVs. These merits are very convenient in calculation environments using a personal computer.

The details of the method of characteristics applied are omitted here because of the space limitation. The details can be found in the Appendix of Yamaguchi [14].

5 .2 Valve transient flow

Transient behaviors of the flow through the valve could be essential as one of the flow-path boundary conditions. Hitherto quasi-steady valve models have often been employed in the field of surge analyses. In consideration of high-pressure-ratio situations across the valve in multistage compressor systems or plants, however, some model allowing for situations including compressibility effects and possible supercritical pressure ratios, etc., in addition to the flow resistance effects, would be indispensable. Here, a valve model, which is simple but is promising to be adaptable to various situations, is tried to apply.

The flow situation is assumed roughly as that in a narrow passage having a valve opening area Av and a length of ΔLv, as shown in Fig. 7. When the mass contained in the valve flow CV is assumed to move together, the following relation results from consideration of forces and momentums;

$$\Delta L_V \frac{\partial W_V}{\partial t} = A_V (p_1 - p_2) - W_V (v_2 - v_1) - R_V \tag{18}$$

Here, Wv: mass flow through the valve, Rv: resistance force in the passage, v: flow velocity. Suffices 1 and 2: inlet and exit of the CV, respectively.

The above equation could be simplified as follows; The flow resistance force is very roughly expressed as follows,

$$R_V = \xi_V (1/2) W_V v_2 \tag{19}$$

Here, ξv: valve resistance factor.

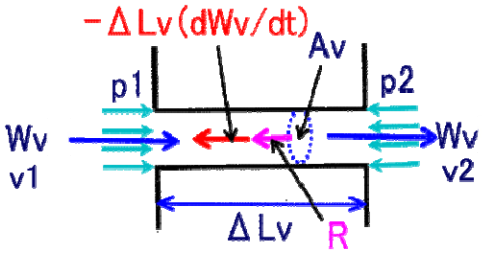

Fig. 7 Flow situations through a valve passage

The second and the third groups of terms in the right-hand side of Eq. (18) could be arranged as follows;

$$-W_V\left[\, v_2\left(1+\frac{1}{2}\xi_V\right) - v_1 \,\right] = -W_V v_1\left[\left(\frac{v_2}{v_1}\right)\left(1+\frac{1}{2}\xi_V\right) - 1\right] \approx -\frac{W_V^2}{A_V \rho_1}\left[\left(\frac{p_1}{p_2}\right)^{1/n}\left(1+\frac{1}{2}\xi_V\right) - 1\right] \tag{20}$$

Here, a polytropic change with polytropic index n was assumed for the flow through the valve passage.

$$(\frac{v_2}{v_1}) \approx (\frac{\rho_1}{\rho_2}) \approx (\frac{p_1}{p_2})^{1/n} \tag{21}$$

And α_{V0} is used as a factor considering the effects of the pressure ratio and the resistance force, as follows;

$$\alpha_{V0} = 1 \Big/ \left[\left(\frac{p_1}{p_2} \right)^{1/n} \left(1 + \frac{1}{2} \xi_V \right) - 1 \right] \tag{22}$$

Then Eq. (17) could be simplified further as follows;

$$\Delta L_V \frac{\partial W_V}{\partial t} = A_V (p_1 - p_2) - \frac{1}{\alpha_{V0}} \frac{W_V^2}{A_V \rho_1} \tag{23}$$

Then, in the steady-state condition immediately before the static stalling point, the following relation gives the apparent valve opening area *Avo* as the one that allows to pass the initial stalling mass flow W_V for the valve pressure difference $(p_1 - p_2)$.

$$A_{V0} = W_V / \sqrt{\alpha_{V0} \rho_1 (p_1 - p_2)} \tag{24}$$

In the above, α_{vo} is assumed as a constant value prior to the steady-state stalling. Since α_{vo} is naturally dependent on the pressure ratio and the resistance force factor across the valve, it might be changeable during the surge cycle. In order to take into account the situation, the following Eq. (25) is assumed to hold very approximately by introducing an empirical adjusting factor β_V.

$$\Delta L_V \frac{\partial W_V}{\partial t} = A_V (p_1 - p_2) - \frac{\beta_V}{\alpha_{V0}} \frac{W_V^2}{A_V \rho_1} \tag{25}$$

The length of the valve flow-path is assumed to be expressed as follows;

$$\Delta L_V = \varepsilon_V \sqrt{A_{V0}} \tag{26}$$

Here, ε_V is an empirical factor for the passage length.

Valve flow transient situation could be evaluated by Eq. (25) by the initial valve opening area A_{Vo} and by assumed values of β_V and ε_V.

The above formulation could or should be modified reasonably in accordance to the possible situations such as, for example, in super-critical pressure-ratio conditions. At present, the author assumes the simplest condition of constant values of α_{V0}, β_V and ε_V.

6. Experimental surge behaviors compared with SRGTRAN results

SRGTRAN has not finished a thorough experimental validation, i.e. comparison of the analytical results with actual surge behaviors, because of unavailability of consistent and detailed information on surge and its hardwares concerning multistage high-pressure-ratio compressors. Some trial analyses, however, have suggested that the analytical results could suitably describe and explain surge behaviors in accordance with our experiences (Yamaguchi [10, 11, 14, 22]).

An example of surge data which was obtained experimentally in a closed-loop flow-path is given below and is compared with some corresponding analytical results by SRGTRAN concerning a similar but much simplified situation.

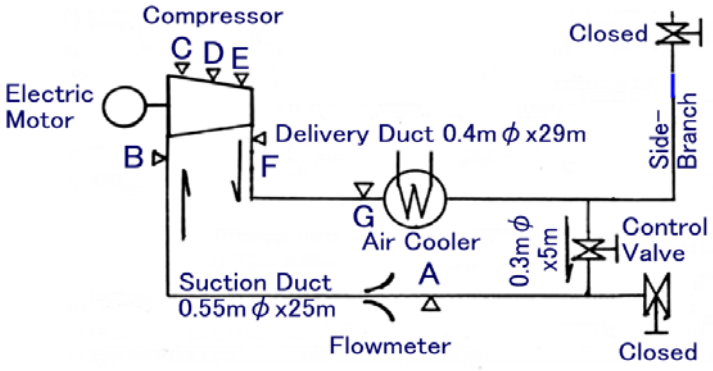

Fig. 8 The compressor and duct system showing the surge phenomena in Fig. 9

6.1 Experimental observations at a compressor in a closed-loop flow-path

In an experimental closed-loop flow-path shown schematically in Fig.8, surge behaviors shown in Fig. 9 were observed (Ref. [21]). The compressor has the dimensions given in Table 1. It is a nine-stage axial flow compressor having a design pressure ratio of 3.82 at 11300 rpm. The flow-path was rather complicated in that it had an air-cooler, a met-

ering nozzle, and a very long side-branch duct branched from the trunk-line as is shown toward the top right area in Fig. 8. Its other end is closed. The compressor delivery pressure was kept nearly at the atmospheric pressure.

The surge behaviors shown in Fig. 9 were obtained at the compressor speed of 10700rpm. The stalling pressure ratio was 4.0. The oscillograms identified as A – G in Fig. 9 were measured at the locations indicated in Fig. 8. Point A was located in the suction flow-path, B in the compressor suction chamber, C in front of the first rotor row in the compressor annulus flow-path, F in the delivery chamber, and G in the delivery flow-path.

In the stalling phase of the surge cycles, pressures at A, B, and C in the suction flow-path are seen to increase as indicated by P1 and in the unstalling phase they fall as indicated by P2. Here, it should be noted that the oscillogram "Ps at C" has positive sign downward. Pressures at F and G in the delivery flow-path are seen to show a reversed manner. They tend to drop in the stalling phase as P3 and to rise as P4 and P5 in the unstalling phase. Higher-frequency oscillations are superposed on them. The behaviors are quite different from those seen in the ordinary flow-path conditions with an open inlet and a throttled exit. The oscillogram "V at B" indicates the output signal of a hot-wire anemometer mounted at B in the suction chamber. The flow at B in the suction chamber shows an abrupt stop of flow at the stalling point and then a continued stagnation as is indicated by W1. It recovers as indicated by W2, but the flow recovery shows some time lag as indicated by an arrow W3 compared with the pressure recovery time. Then the flow tends to slow down toward the re-stalling as indicated by W4.

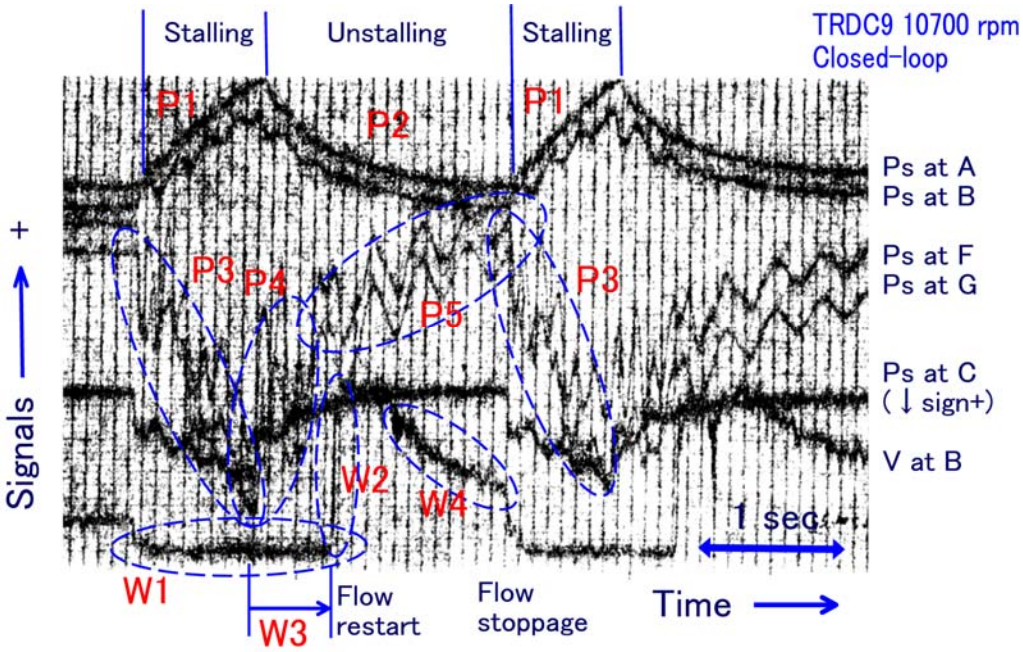

Fig. 9 An example of surge phenomena in an experimental compressor in a closed-loop duct with the delivery pressure nearly atmospheric (Ps at C has a reversed sign)

The surge frequency is read to be 0.39 (Hz)

6.2 A trial of analysis for the example

(a)The compressor and the flow-path for the analysis Main numerical figures of the compressor are given in Table 1. The stage characteristics given in Fig. 10 has been assumed for the analysis for each stage. It has been determined on the experimental data in the sound zone and supposed in the stalled zone from literature survey results (*cf* Greitzer [3], Gamache and Greitzer [15], Day, Greitzer, and Cumpsty [16], Davis, Jr. and O'Brien [6], etc.).

The flow-path geometry for the analysis, i.e., the sectional area distribution *A* along the flow-path is given in Fig. 11 for x coordinate from the suction duct inlet. It approximates roughly the experimental flow-path shown schematically in Fig. 8, but the details have been much simplified and the branched long duct shown in Fig.8 has been omitted.

The attached numerical numbers in Fig. 11 show corresponding numbers of the CVs constituting the flow-path. Numbers 1 and 61 are the inlet and the exit, respectively, which are joined together with a valve for simulation of the closed-loop flow-path situation. The compressor exists between 26 and 27, and a heat exchanger (an air cooling unit) is assigned at CV 45.

Table 1 Dimensions of the Experimental Compressor

Type	Axial Flow Compressor
Stages	9
Tip diameter of the first stage *Dt1* (m)	0.508
Hub diameter *Dh* (m)	0.356
Design speed (rpm)	11300(288.2K)
Design flow (m^3/s)	11.5
Design pressure ratio	3.82 (288.2K)
RPM for analysis	100% design speed (313.2 K)
Stage characteristics	Identical for all stages

(b)The analytical surge behavior The analyses have been conducted at 10700 rpm near 95 % design rpm. The initial condition immediately before stalling has the suction pressure and temperature about 27 kPa Abs. and 313.2 K, and the delivery pressure nearly atmospheric one, i.e., 101.3 kPa Abs. The pressure ratio is 3.9. The situation is corresponding approximately to the above experimental one.

Figure 12 shows the analytical surge behaviors in the closed-loop flow-path where the abscissa is time in terms of time step number *k*. Figure 12(a) and (b) show behaviors of pressure *Ps* and mass flow *W*, respectively. Attached integers show respective

CV numbers shown in Fig. 11. The air cooler is located at CV No. 45 and sets the heat absorption rate to give the leaving flow temperature of 313.2 (K).

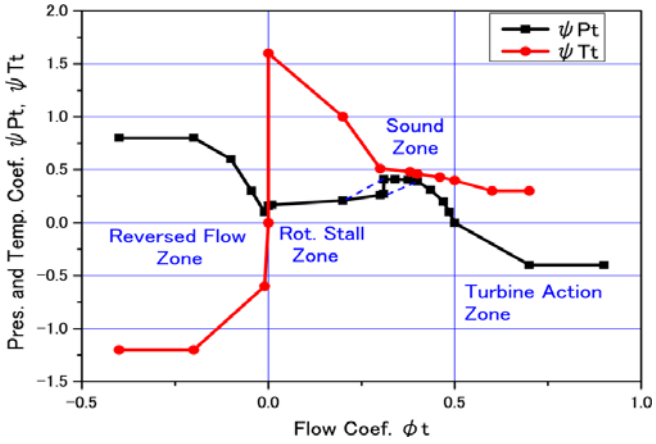

Fig. 10 Wide–range stage characteristics assumed for the compressor stages

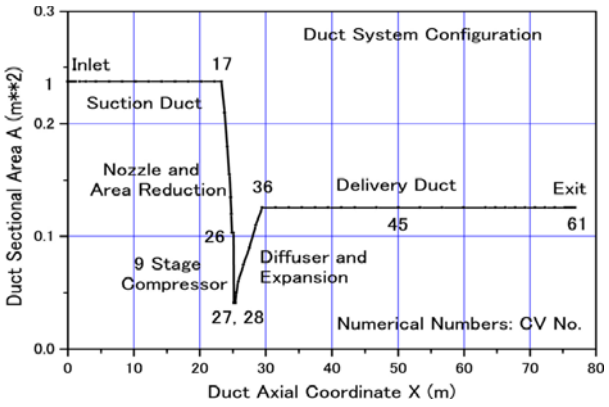

Fig. 11 Distribution of the flow path sectional area against the duct axial coordinate and the control volume numbers. Inlet and exit are connected by a valve.

Following flow behaviors are observed. In Fig. 12(a), in the stalling phase, the suction pressure tends to rise and the delivery pressure to lower. In the unstalling phase, in contrast, the suction pressure tends to lower and the delivery pressure to rise. As a whole, the surge pressures approach an averaged level from both sides of the pressures in the suction and the delivery. The mass flow behaviors shown in Fig. 12(b) indicate the antinode of the variation in the midstream zone including the compressor (CV No. 26 and 27). It suggests the fundamental mode of the mass flow having a half-wavelength with its node at the valve.

These variations are quite different from those observed usually in the flowpaths either with an open inlet and a throttled exit or with a throttled inlet and an open exit, both of which tend to show near a quarter-wavelength oscillations. The resulting surge frequency is read to be 0.49 (Hz).

Some other information such as working conditions of each stage, etc. are given in Yamaguchi [22].

(c)Comparison between the experimental results and the analytical one Some characteristic zones, indicated by tags P1-P5, W1 - W4, are shown with the same letters both in Fig. 12 and Fig.9. Suction pressure behaviors for P1 and P2 both in Figs. 12 and 9 show very similar tendencies. Delivery pressure behaviors for P3, P4 and P5 both in Figs. 12 and 9 show similar tendencies also, but the experimental ones show somewhat more oscillatory behaviors. The presence of the long branched duct in the actual flow-path could have affected these differences and also the difference in

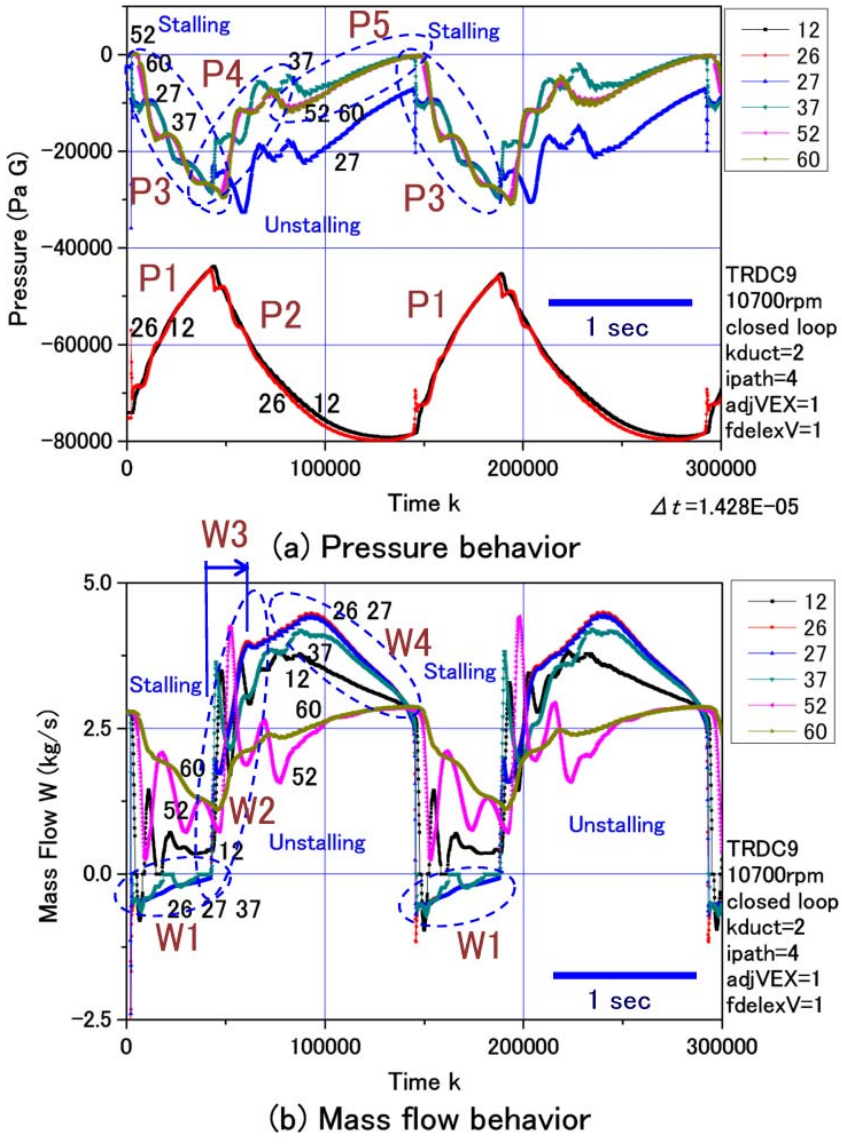

Fig. 12 Simulated surge phenomena in the closed-loop duct

the surge cycle times. The flow speed for W1 shows the flow stagnation or reversal during the stalling or stalled phase. W2 shows that the mass flow recovery in the neighborhood of the compressor started with some time lag in comparison with the pressure recovery indicated by W3. Then the flow tends to reach at a peak and then slow down toward the re-stalling as indicated by W4 both in Figs. 12 and 9. These behaviors are seen very similar between the analytical results in Fig.12 and the experimental observations in Fig. 9.

Concerning the apparent time lag W3, inspections of analytical results on the stage working conditions (Yamaguchi [18]) suggest the following process. The real unstalling in the mass flow is established by the condition that all stages have come back into the sound zone. However, immediately after the return from the reversed flow condition, the situation has only reached at the one with front stages yet deep in the stalled zone of very low flow coefficient and with rear stages in the turbine-action zone of very high flow coefficient. Thus the complete flow recovery lags in time compared with the instant of pressure un-stalling. The rather slow increase in the flow shown by W2 in Fig. 12(b) suggests the situation. On the other hand, W2 in Fig. 9 shows an abrupt flow increase and a clear time lag in the experimental situation. Both observations are considered to mean the same phenomenon, although somewhat different in appearance. The time lags have often been experienced in actual multi-stage compressors.

Thus, the above time lag W3 could be said to have no direct relation with time lags τ_{lagP} and τ_{lagT} used in Eqs. (10) and (11). The latters are of the order of magnitude of one revolution time of the rotor, i.e., about 0.006 (s) here, in contrast to W3 of about 0.26 (s) and 0.55 (s) observed in Fig. 12(b) and Fig. 9, respectively.

Table 2 shows a rough comparison of the analytical results with the experimental one. The analytical surge frequency is larger by about 20% than the experimental one, which might be attributed to the absence of the long side-branch duct in the analytical flow-path. The pressure amplitudes are seen to be comparable in the order of magnitude between both.

The above comparison, though rather qualitative, shows that the analytical results could predict the experimental surge behaviors fairly well even in the rather complicated situation of the closed-loop flow-path. It could be said that these similarity suggests the validity of the analysis by SRGTRAN.

Table 2 Qualitative comparison of the surge wave data between the experimental result and the analytical one

	Experimental	Analytical	
Surge Period *Ts* (s)	2.55	2.05	Analytical/Experimental Ratio: 0.8
Surge Frequency *fs* (Hz)	0.39	0.49	Analytical/Experimental Ratio : 1.26
Stalling Period Time Ts_1(s)	0.85	0.57	
Unstalling Period Time Ts_2 (s)	1.7	1.48	
Ts_1/Ts	0.33	0.28	
Time Lag W3 in Flow Recovery (s)	0.55	0.26	
Suction Pressure Rise in the Stalling Period (kPa)	34.5	31-34	Comparable
Delivery Pressure Drop in the Stalling Period (kPa)	34.5	30-35	Comparable

7. Conclusion

The outline of a surge transient analysis and simulation code SRGTRAN is described. Experimental surge behaviors in a nine-stage compressor in a closed-loop flow- path are picked up as an example, and an analysis about the setup was conducted on the basis of simplified approximate data on the compressor and the flow- paths. Comparison of the analytical results by SRGTRAN with the experimental surge data has shown good qualitative agreement, although in a limited scope. It is believed that the analysis method could now be used successfully, although some more experimental verifications and polish- ups, and accumulation of experimental adjustments and corrections are desired.

Nomenclature

A	Sectional area of flow-path (m^2)	W	Mass flow (kg/s)
A_m	Average sectional area of CV (m^2)	W_V	Mass flow through a valve (kg/s)
A_V	Valve opening area (m^2)	x	axial coordinate along the flow-path (m)
a	Speed of sound (m/s)	α_V	Adjusting factor of valve passage flow
b	Source term in Eqs.(15) ~ (17)	β_V	Adjusting factor of valve passage flow
C_P	Specific heat at constant pressure (J/kg/K)	ΔL_V	Length of valve flow passage (m)
C_V	Specific heat at constant volume (J/kg/K)	Δt	Time increment (s)
Enet	Net stage work (J)	Δx	x increment (m)
f	Variable of x in Eqs.(15)~(17)	Δx^*	Axial length of CV(stage) (m)
fs	Surge frequency (Hz)	ε_V	Length factor of valve flow passage
Fnet	Net stage axial force (N)	κ	Ratio of specific heats
i	CV number in the flow-path	ρ	Density of flow (kg/m^3)
J, j	Compressor stage number	τ_{lagP}	Time lag in stage force (s)
k	Time step number	τ_{lagT}	Time lag in stage work (s)

k_{bk}	Blockage factor	φ	Stage flow coefficient
n	Polytropic index	ψ_P	Stage pressure coefficient
ps	Static pressure (Pa)	ψ_T	Stage temperature-rise coefficient
P_{T1}	Total pressure at the stage inlet (Pa)		
P_{T2}	Total pressure at the stage exit (Pa)	**subscript**	
R_V	Resistance force in valve flow passage(N)	1	Inlet of CV or stage
Tadj	Coefficient of CFL condition	2	Exit of CV or stage
Ts	Surge period (s)	Exit	Exit of the duct system
Ts_1	Stalling period in surge (s)	i	Axial location in the duct system
Ts_2	Unstalling period in surge (s)	k	Time point
T_{T1}	Total temperature at the stage inlet (K)	m	Mid position of the stage or CV
T_{T2}	Total temperature at the stage exit (K)	V	valve
u	Flow velocity, axial velocity (m/s)		
u	Variable of t in Eqs.(15)~(17)	**superscript**	
$Uref$	Reference speed of compressor (m/s)	*	Steady-state value of the compressor condition

References

[1] Fujii, S., 1947, "Stability and Surging in Centrifugal Pumps, Part 1 and Part 2 (in Japanese)," Transaction, Japan Society of Mechanical Engineering, Vol. 13, No. 44, 1947-5, pp. 184-191and 192-201.

[2] Katto, Y., 1960, "Some Fundamental Natures of Resonant Surge, 1st Report and 2nd Report (in Japanese)," Vol. 26, No. 162, 1960-2, pp. 256-264 and pp. 265-273.

[3] Greitzer, E. M., 1976, "Surge and Rotating Stall in Axial Flow Compressors, Part I and II," ASME, Journal of Engineering for Power, Vol. 98, 1976-4, pp. 190-198 and 199-217.

[4] Corbett, A.G., and Elder, R.L., 1976, "Mathematical Modeling of Compressor Stability in Steady and Unsteady Flow Conditions," Paper 12, AGARD-CP-177.

[5] Chamblebee, C.E., Davies, Jr., M.W., and Kimzey, W.F., 1980, "A Multi-Stage Axial Flow Compressor Mathematical Modeling Technique with Application to Two Current Turbofan Compression Systems," AIAAPaper, AIAA-80-0054.

[6] Davies, Jr., M.W., and O'Brien, W.F., 1987, "A Stage-by-Stage Post-Stall Compression System Modeling Technique," AIAA-87-2088.

[7] Schobeiri, M.T., Attia, M., and Lippke, C., 1994, "GETRAN: A Generic Modularly Structured Computer Code for Simulation of Dynamic Behavior of Aero- and Power Generation Gas Turbine System," Journal of Engineering for Gas Turbine and Power, Transaction of the ASME, Vol. 116, 1994-7, pp. 483-494.

[8] Badmus, O.O, Chowdhury, S., Eveker, K.M., and Nett,C.N., 1995, "Control-Oriented High-Frequency Turbomachinery Modeling: Single-Stage Compressor System One-Dimensional Model," Journal of Turbomachinery, Transaction of the ASME, Vol. 117, 1995-1, pp. 47-61.

[9] Schobeiri, M., 2004, "Turbomachinery Flow Physics and Dynamic Performance," Springer.

[10] Yamaguchi, N., 2012, "A Study on the Stagnation-Stall Boundaries Based on Analytically-Evaluated Surge Conditions in Axial Flow Compressors," No. ISUAAAT13-S5-1, The 13th International Symposium on Unsteady Aerodynamics, Aeroacoustics and Aeroelasticity of Turbomachinery, 2012-9.

[11] Yamaguchi, N., 2013, "Analytical Study on Stall Stagnation Boundaries in Axial Compressor and Duct System," International Journal of Fluid Machinery and Systems, Vol. 6, No. 2, April-June 2013, pp.56-74.

[12] Editing Committee of CFD, 1995, "Analysis of Compressible Flows (in Japanese)," Computational Fluid Dynamics Series, Vol.2, Tokyo University Press, pp. 40, and 54-55.

[13] Tanahashi, T., 1993, "Dynamic Features in Flow-paths (3) (in Japanese)," Sciences of Machines, Vol. 45, No. 10, pp.1059-1060.

[14] Yamaguchi, N., 2011, "Surge Transient Flow Phenomena in a Multistage Axial Flow Compressor-Duct System Predicted by a Stage-by-Stage Simulation Method, Part I Development of Simulation Code "SRGTRAN" (in Japanese)," Research Bulletin of Faculty of Sciences and Engineering, Meisei University, No. 47, 2011-3, pp. 73-85.

[15] Gamache, R.N. and Greitzer, E.M., 1986, "Reverse Flow in Multistage Axial Compressors," AIAA-86-1747, 1986-6.

[16] Day, I.J., Greitzer, E.M., and Cumpsty, N.A., 1978, "Prediction of Compressor Performance in Rotating Stall, Journal of Engineering for Power," ASME, Vol. 100, No.1, 1978-1, pp. 1-14.

[17] Hosny, W.M. and Steenken, W.G., 1986, "Aerodynamic Instability of an Advanced High-Pressure-Ratio Compression Component," AIAA-86-1619.

[18] Boyer, K.M. and O'Brien, W.F., 1989, "Model Prediction for Improved Recoverability of a Multistage Axial-Flow Compressors," AIAA-89-2687.

[19] Copenhaver, W.W. and Okiishi, T.H., 1989, "Rotating Stall Performance and Recoverability of a High-Speed 10-Stage Axial-Flow Compressors," AIAA-89-2684.

[20] Bloch, G.S., and O'Brien, W.F., 1992, "A Wide-Range Axial-Flow Compressor Stage Performance Model," ASME 92-GT-58.

[21] In-house data of Mitsubishi Heavy Industries, Limited

[22] Yamaguchi, N., 2103, "Analytical Study on Effects of Flow Path Layouts on the Compressor Surge Phenomena (in Japanese)," Turbomachinery, Turbomachinery Society of Japan, Vol. 41, No. 2 (2013-2), pp. 89-97.